



## Molecular and cellular pharmacology

## 2,2'-Fluorine mono-carbonyl curcumin induce reactive oxygen species-Mediated apoptosis in Human lung cancer NCI-H460 cells



Guo-Yun Liu, Qiang Zhai, Jia-Zhuang Chen, Zhuo-Qing Zhang, Jie Yang\*

School of Pharmacy, Liaocheng University, 1 Hunan Street, Liaocheng, Shandong 252000, China

## ARTICLE INFO

## Article history:

Received 8 May 2016

Received in revised form

27 May 2016

Accepted 3 June 2016

Available online 4 June 2016

## Keywords:

Curcumin analogs

Fluorine

Reactive oxygen species

Apoptosis

## ABSTRACT

In this paper, we synthesized three fluorine-substituted mono-carbonyl curcumin analogs and evaluated their cytotoxicity against several cancer cells by the MTT assay. The results exhibited that all the three compounds were more active than the leading curcumin. Especially, 2,2'-F mono-carbonyl curcumin, **1a**, surfaced as an important lead compound displaying almost 4-fold cytotoxicity relative to curcumin. More importantly, **1a** was more stable in (RPMI)-1640 medium and more massive uptake than curcumin, which may be relationship to their cytotoxicity, apoptotic activity and reactive oxygen species generation. And then, the generation of reactive oxygen species can disrupt the intracellular redox balance, induce lipid peroxidation, cause the collapse of the mitochondrial membrane potential and ultimately lead to apoptosis. The results not only suggest that 2,2'-F mono-carbonyl curcumin (**1a**) may cause cancer cells apoptosis through reactive oxygen species-Mediated pathway, but also gives us an important information for design of mono-carbonyl curcumin analog.

© 2016 Elsevier B.V. All rights reserved.

## 1. Introduction

Curcumin is a naturally occurring phenolic compound as a yellow pigment obtainable from rhizomers (turmeric) of perennial herb *Curcuma longa* Linn. It has been show spectral physiological and pharmacological activity including antiinflammatory (Fu et al., 2008), antibacterial (Baldwin et al., 2015), antioxidant (Gazal et al., 2014) and anticancer activity (Chen et al., 2016). Of particular interest is the anticancer property of curcumin, which has been the focus of hundreds of publications including several comprehensive reviews (Červinková et al., 2009; Ravindran et al., 2009; López-Lázaro, 2008; Reuter et al., 2008; Kunnumakkara et al., 2008). Curcumin suppress proliferation and/or induce apoptosis of cancer cells through modulating a variety of molecular targets in the development of cancer (Alexandrow et al., 2012; López-Lázaro, 2008; Reuter et al., 2008). Interestingly, curcumin has been demonstrated to preferentially trigger apoptosis in transformed cells in vitro while apparently sparing their normal counterparts (Syng-ai et al., 2004). Additionally, phase I clinical trials have concluded that curcumin could be administered at up to 8 g/day without any side effects (Cheng et al., 2001). Curcumin's significant anticancer activity, along with its low molecular weight and lack of toxicity, makes this molecule an ideal candidate for development of cancer chemoprevention and chemotherapy

agents. Unfortunately, preclinical and clinical studies have suggested its poor bioavailability and pharmacokinetic profiles, which was due to its low absorption, rapid metabolism, and rapid systemic elimination (Anand et al., 2007; Sharma et al., 2007). Another possible reason for the low bioavailability of curcumin is its instability under physiological conditions, which lead to extensive effort to continuously devote to the synthesis of new curcumin analogs with the aim of improving the flaws and enhancing anticancer activity of the parent compound (Anand et al., 2008; Agrawal et al., 2010; Adams et al., 2004, 2005; Amolins et al., 2009; Liang et al., 2009).

It is believed that the  $\beta$ -diketone moiety of curcumin contributes to its instability under physiological conditions, and induces rapid degradation and metabolism of curcumin (Anand et al., 2007; Sharma et al., 2007). A large amount of research work demonstrated that replace the  $\beta$ -diketone moiety by ketone not only enhanced stability in vitro but also greatly improved pharmacokinetic profiles in vivo (Liang et al., 2009). Our group's work was also exploiting reactive oxygen species-promoting signaling for designing curcumin-inspired anticancer agents and found that they can target TrxR (thioredoxin reductase) and convert this antioxidant enzyme into a reactive oxygen species promoter (Dai et al., 2015).

Drug candidates with one or more fluorines have become common place. The special nature fluorine imparts a variety of properties to certain medicines, including enhanced binding interactions, metabolic stability, changes in physical properties, and selective reactivities (Hagmann et al., 2008). In this spirit, we design and synthesized three mono-carbonyl curcumin analogs

\* Corresponding author.

E-mail address: [yangjie1110@163.com](mailto:yangjie1110@163.com) (J. Yang).

with fluorine-substituted groups attaching to 2-, 3- or 4-position on the aromatic ring (Fig. 1). Thus we focus on the SAR (structure-activity relationships) underlying cytotoxicity and explore the apoptotic mechanism associated with curcumin analogs.

## 2. Materials and methods

### 2.1. Materials

Roswell Park Memorial Institute (RPMI)-1640 was from GIBCO. 2',7'-dichlorofluorescein diacetate, rhodamine 123, 3-(4,5-dimethylthiazol-2-yl)-2,5-diphenyltetrazolium bromide (MTT), Glutathione reductase (GR), the reduced (GSH) and oxidized (GSSG) glutathione, N-acetylcysteine (NAC), 2-vinylpyridine (97%) and thiobarbituric acid were obtained from Sigma. All other chemicals were of the highest quality available.

### 2.2. Synthesis of the curcumin analogs

The mono-carbonyl curcumin analogs were synthesized according to the published procedure (Weber et al., 2005). Briefly, Aqueous NaOH (20 wt%, 5 ml) was added dropwise to a vigorously stirred solution of modified benzaldehyde (51 mmol) and ketone (25 mmol) in ethanol (8 ml). After 48 h stirring at room temperature, distilled water (40 ml) was added to the reaction mixture followed by the neutralization with HCl. The precipitating yellow solid was filtered off, washed with distilled water and dried under vacuum. The crude products were directly charged onto a silica gel column and eluted with a mixture of ethyl acetate/petroleum to afford the pure product. Their structures were confirmed by  $^1\text{H}$  and  $^{13}\text{C}$  NMR spectroscopy.

#### 2.2.1. 1,5-Bis(2-fluorophenyl)-penta-1,4-dien-3-one (1a)

Yellow solid; m.p.: 65–69 °C; Yield: 71.4%;  $^1\text{H}$  NMR (400 MHz,  $\text{CD}_3\text{Cl}$ ),  $\delta$  7.85 (d,  $J=16.4$  Hz, 2 H), 7.62 (dt,  $J=7.6, 1.6$  Hz, 2 H), 7.37–7.42 (m, 2 H), 7.12–7.23 (m, 6 H);  $^{13}\text{C}$  NMR (100 MHz,  $\text{CD}_3\text{Cl}$ ),  $\delta$  189.0, 162.9, 160.4, 136.1, 131.9, 129.4, 127.6, 124.5, 122.9, 116.4.

#### 2.2.2. 1,5-Bis(3-fluorophenyl)-penta-1,4-dien-3-one (1b)

Yellow solid; m.p.: 93–95 °C; Yield: 62%;  $^1\text{H}$  NMR 400 MHz ( $\text{CD}_3\text{Cl}$ ),  $\delta$  7.68 (d,  $J=16.0$  Hz, 2 H), 7.60–7.63 (m, 4 H), 7.10 (t,  $J=7.6$  Hz, 4 H), 6.98 (d,  $J=16.0$  Hz, 2 H);  $^{13}\text{H}$  NMR 100 MHz ( $\text{CD}_3\text{Cl}$ ),  $\delta$  188.4, 165.3, 162.8, 142.1, 131.0, 130.3, 125.1, 116.3, 116.0.

#### 2.2.3. 1,5-Bis(4-fluorophenyl)-penta-1,4-dien-3-one (1c)

Yellow solid; m.p.: 147–149 °C; Yield: 71%;  $^1\text{H}$  NMR 400 MHz ( $\text{CD}_3\text{Cl}$ ),  $\delta$  7.69 (d,  $J=16.0$  Hz, 2 H), 7.55 (d,  $J=8.7$  Hz, 4 H), 6.89 (d,  $J=8.7$  Hz, 4 H), 6.64 (d,  $J=15.9$  Hz, 2 H), 5.98 (s, 1 H);  $^{13}\text{H}$  NMR 100 MHz ( $\text{CD}_3\text{Cl}$ ),  $\delta$  184.6, 160.6, 141.1, 131.0, 127.7, 122.1, 116.9, 101.8.

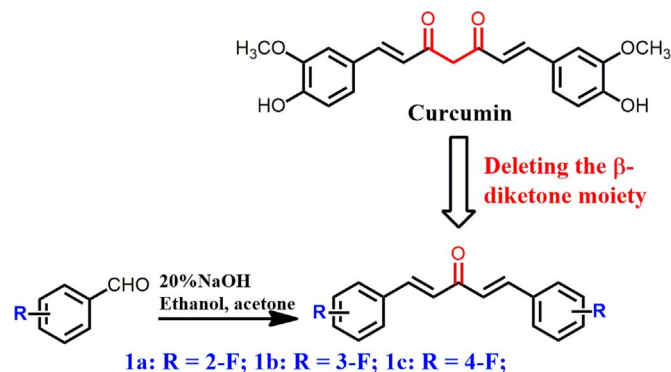


Fig. 1. Molecular structures of curcumin and its analogs.

### 2.3. Cell culture

Human lung cancer cells (NCI-H460), Human lung carcinoma cells (A549), Human liver hepatocellular carcinoma (HepG2) and normal liver cells (Chang'sliver) were purchased from the Shanghai Institute of Biochemistry and Cell Biology, Chinese Academy of Sciences and cultivated in RPMI 1640 at 37 °C in a humidified atmosphere with 5%  $\text{CO}_2$ .

### 2.4. MTT assay

Cell viability was determined by a colorimetric assay using MTT. NCI-H460, HepG2, A549 and Chang'sliver cells were seeded at a density of  $3 \times 10^3$ /well in a complete growth medium in 96-well plates and incubated for 24 h. Then cells were treated for another 24 or 48 h with compounds at the selected concentration before the MTT assay.

### 2.5. Stability assay

Stability of curcumin and **1a** (25  $\mu\text{M}$ ) in RPMI 1640 supplemented with 10% (v/v) heat-inactivated fetal calf serum at 25 °C (The common international guideline for long-term stability studies specifies  $25 \pm 2$  °C (ICH, Q1A(R2), 2003)) was monitored at their band maximum for 150 min (at 10-min intervals) by using UV/Vis spectroscopy.

### 2.6. Cell apoptosis analysis

NCI-H460 cells ( $5 \times 10^5$ /well) were plated in six-well plates and incubated for 24 h to allow exponential growth, then treated with the test compounds for 24 h at the indicated concentration. When necessary, the cells were pretreated with GSH or NAC for 1 h before adding test compounds. The treated cells were harvested and labeled with annexin V-FITC/PI. A total of 10,000 cells per sample were collected and analyzed by FACSDiva software.

### 2.7. Intracellular reactive oxygen species measurement

Generation of reactive oxygen species was measured by the oxidative-sensitive fluorescent probe DCFH-DA. After 6 of treatment with the test compounds in the absence or presence of GSH or NAC, NCI-H460 cells were incubated with 3  $\mu\text{M}$  DCFH-DA for 30 min at 37 °C in the dark. Then cells were washed with PBS and analyzed immediately for 2',7'-dichlorofluorescein fluorescence intensity by flow cytometry.

### 2.8. Uptake and metabolic stability assay

NCI-H460 cells were seeded in six-well plates at a density of  $5 \times 10^5$  cells/well and incubated for 24 h. After 0.5, 1, 2, 4 or 6 h of treatment with the test compounds, the cells were extracted with ice-cold methanol (1 ml/well) for 10 h at 4 °C. Then the suspension was centrifuged for 5 min (9400 g, at 4 °C), and the supernatant was then scanned using a UV/Visible spectrophotometer (Dai et al., 2015).

### 2.9. Measurement of GSH and GSSG levels

NCI-H460 cells at a density of  $5 \times 10^5$  per well were grown in six-well plates for 24 h, after 6 h of treatment with **1a** at the indicated concentrations, the cells were collected, resuspended in 500  $\mu\text{l}$  of ice-cold HCl (10 mM) and lysed by three cycles of freezing and thawing. The remaining protein was subsequently precipitated by adding 120  $\mu\text{l}$  of ice-cold 5-sulfosalicylic acid (SSA, 6.5%, w/v) for 10 min and removed by centrifugation for 15 min (8000 g, at 4 °C). The resulting supernatant was

collected and assayed for total GSH and GSSG according to the glutathione reductase-DTNB recycling assay as described previously (Vandeputte et al., 1994).

### 2.10. Determination of thiobarbituric acid-reactive substance (TBARS)

Lipid peroxidation was measured according to the protocol as described previously (Dai et al., 2015). NCI-H460 cells were seeded at a density of  $5 \times 10^5$  per well in six-well plates and allowed to grow for 24 h, after exposure to **1a** at the indicated concentrations (0, 5, 10, 20 and 30  $\mu\text{M}$ ) for 18 h, the cells were harvested. Then the cells were resuspended in 200  $\mu\text{l}$  ice-cold water and lysed by three cycles of freezing and thawing. The absorbance of resulting supernatants was read at 532 nm, and lipid peroxidation was expressed as MDA equivalence (pmol MDA/mg protein).

### 2.11. Analysis of mitochondrial membrane potential

Mitochondrial membrane potential was monitored by the fluorescent dye, Rhodamine 123. Briefly, NCI-H460 cells ( $5 \times 10^5$ /well) were plated in six-well plates and treated with the test compounds at the indicated concentration for 18 h in the absence or presence of GSH or NAC. The treated cells were collected and analyzed immediately for Rhodamine 123 fluorescence intensity by flow cytometry.

## 3. Results

### 3.1. Cytotoxicity and SAR

We started our studies with a comparison of the cytotoxicity of curcumin with its analogs on several cancer cells and normal Chang's liver cells by means of a MTT-based viability assay. The  $\text{IC}_{50}$  values reported in the Table 1 allowed us to identify the following SAR: (1) The cell-killing effects of the mono-carbonyl curcumin analogs were stronger than that of the leading curcumin. Especially, **1a** surfaced as an important lead compound displaying almost 4-fold cytotoxicity relative to curcumin against NCI-H460 cells. This result may be related to that **1a** in RPMI 1640 supplemented with 10% (v/v) heat-inactivated fetal calf serum was more stable than curcumin (Fig. 2). (2) After treatment for 48 h, the curcumin analogs with the *ortho*-substituent on the aromatic ring(s) was more active than their corresponding *meta*-substituted compounds, which was more active than the *para*-substituted compounds, against the three cancer cells. The presence of the substituents at the *ortho*, but not *para* or *meta*, positions of the aromatic ring(s) significantly increase the cytotoxicity, highlighting a so-called *ortho* effect (Dai et al., 2015). Previously, the presence of *ortho* effect was also proved to significantly

**Table 1**  
Cytotoxicity of curcumin and its analogs against cancer and normal cells.

Comps.	Cytotoxicity for 24 h	Cytotoxicity for 48 h			
		NCI-H460 ( $\text{IC}_{50}/\mu\text{M}^a$ )	A549 ( $\text{IC}_{50}/\mu\text{M}$ )	HepG2 ( $\text{IC}_{50}/\mu\text{M}$ )	Chang's Liver ( $\text{IC}_{50}/\mu\text{M}$ )
<b>1a</b>	106.1 $\pm$ 6.5	11.3 $\pm$ 0.7	17.0 $\pm$ 0.3	26.9 $\pm$ 2.8	11.0 $\pm$ 0.8
<b>1b</b>	125.3 $\pm$ 3.6	17.3 $\pm$ 1.2	35.6 $\pm$ 1.6	> 100	29.0 $\pm$ 1.3
<b>1c</b>	142.3 $\pm$ 2.3	36.7 $\pm$ 2.1	> 100	> 100	38.8 $\pm$ 1.5
<b>Curcumin</b>	88.0 $\pm$ 5.6	41.0 $\pm$ 1.1	51.8 $\pm$ 2.6	52.3 $\pm$ 1.1	29.6 $\pm$ 0.6

<sup>a</sup> The  $\text{IC}_{50}$  value is the concentration of a compound tested to cause 50% inhibition of cell viability after treatment, and is expressed as the mean  $\pm$  S.D. for three determinations.

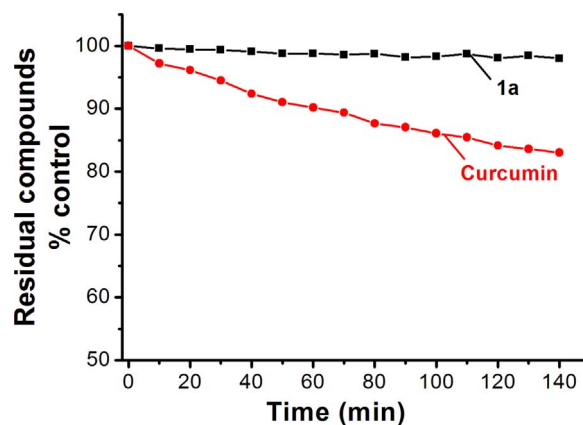


**Fig. 2.** Stability assessment on curcumin (25  $\mu\text{M}$ ) and **1a** (25  $\mu\text{M}$ ) in RPMI 1640 supplemented with 10% (v/v) heat-inactivated fetal calf serum at 25  $^{\circ}\text{C}$  by monitoring the decrease in their maximum absorbance.

strengthen the cytotoxicity of cinnamaldehydes (Chew et al., 2010), chalcones (Gan et al., 2013) and mono-carbonyl curcumin analogs (Dai et al., 2015). (3) **1a** showed less active than curcumin after treatment for 24 h against NCI-H460 cells, which was apposed to the results of 48 h. The phenomenon may be due to the cellular uptake of **1a** and curcumin in NCI-H460 cells. Unfortunately, curcumin analogs showed stronger selectivity against cancer cells and weaker effect in normal cells.

### 3.2. Induction of apoptosis via reactive oxygen species-dependent pathway

Apoptosis is known to be a very important mechanism involved in the anticancer effect induced by chemotherapeutic agents, so we detected the apoptosis-inducing activity of **1a** using flow cytometry. It was found that **1a** was a potent inducer of apoptosis and showed obvious dose-dependent. Specially, after treating NCI-H460 and A549 cells with 30  $\mu\text{M}$  **1a** caused 50.7% and 44.3% late apoptosis, respectively (Fig. 3A and B). Interestingly, pretreatment with the antioxidant, glutathione (GSH) or N-acetylcysteine (NAC), almost completely reversed the apoptosis induced by **1a**, preliminarily indicating the involvement of reactive oxygen species (Fig. 3A and B).

### 3.3. Intracellular reactive oxygen species accumulation

Reactive oxygen species generation has been implicated as an upstream signal that can trigger signaling transduction culminating in apoptosis (Pelicano et al., 2004). In order to measure the capacity of curcumin and its analog to cause intracellular oxidation, we employed the oxidation-sensitive probe, 2',7'-dichlorofluorescein diacetate (DCFH-DA) to measure the intracellular reactive oxygen species levels by flow cytometry. As shown in Fig. 4A and B, **1a** caused a substantial increase in the reactive oxygen species levels in a dose-dependent fashion. Especially, **1a** (30  $\mu\text{M}$ ) induced significantly higher reactive oxygen species accumulation than 30  $\mu\text{M}$  of curcumin (Fig. 4A and B). The high reactive oxygen species-generating ability should be responsible for the better cytotoxicity of **1a**. The results also may indicate a tight link among the reactive oxygen species-generating ability, cytotoxicity and apoptosis-inducing activity. More importantly, pretreatment with glutathione or N-acetylcysteine for 1 h, the reactive oxygen species generation induced by 30  $\mu\text{M}$  **1a** in NCI-H460 and A549 cells was almost completely reduced. The results further indicated that the reactive oxygen species-generating ability of **1a** was closely related to its cytotoxicity and apoptosis-inducing activity.

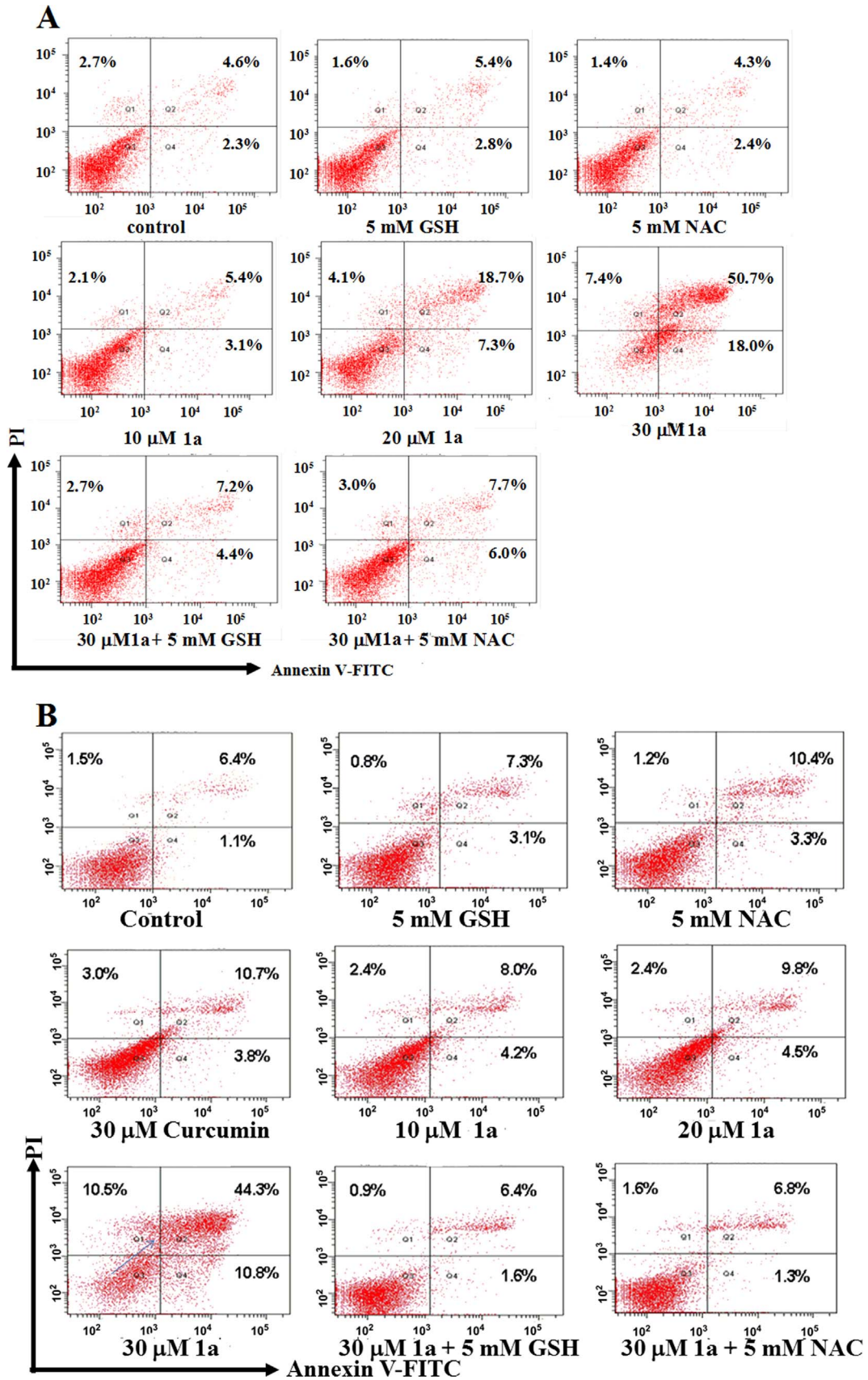


**Fig. 3.** Flow cytometric analysis for apoptosis induction of NCI-H460 (A) or A549 (B) cells after 24 h treatment with curcumin or **1a** at the indicated concentrations in the absence or presence of 1 h pretreatment with GSH or NAC. Percentage of cells in early and late apoptosis and necrosis is indicated in each quadrant. Each experiment was performed in triplicate.

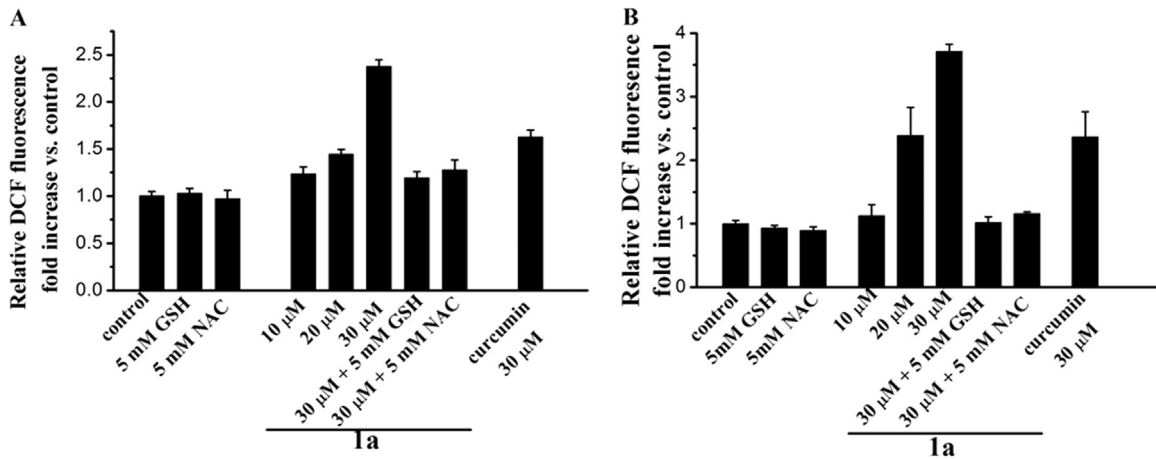


**Fig. 4.** Effects of GSH (5 mM) and NAC (5 mM) on the reactive oxygen species generation induced by **1a** at the indicated concentrations in NCI-H460 (A) or A549 (B) cells. Each experiment was performed in triplicate.

### 3.4. Cell uptake

To further explain the cytotoxicity activity, reactive oxygen species-generating ability and apoptosis-inducing activity of **1a** was stronger than that of leading curcumin, we also compared the cellular uptake of **1a** and curcumin in NCI-H460 cells. As shown in Fig. 5, curcumin was well absorbed to reach a peak value after 30 min of incubation, but it was rapidly and even completely metabolized for 6 h. Nevertheless, **1a** reach a peak value after 1 h of incubation and was fairly stable. This results was in line with the reactive oxygen species-generating ability and the cytotoxicity of curcumin and **1a**. It was also emphasized that incorporating of fluorine group into small molecules could effectively enhance its binding interactions, metabolic stability, changes in physical properties. Take together, the results of the cellular uptake may partly explain why **1a** and curcumin have the opposite cytotoxic activity orders against NCI-H460 cells after treatment for 24 and 48 h.

### 3.5. Determination of redox balance in NCI-H460 cell

A sustained flux of reactive oxygen species usually resulted in an imbalance of intracellular redox state, which was estimated by the ratio of GSH and its disulfide GSSG (Klaunig and Kamendulis, 2004). Therefore, we tested if the reactive oxygen species generation induced by **1a** could cause changes of the ratio of GSH and GSSG. As shown in Fig. 6, the ratios of GSH/GSSG were sharply decreased in a dose-dependent fashion after treatment with **1a** at the indicated concentrations. Particularly, after treatment with 20  $\mu\text{M}$  **1a** for 6 h, the ratio of GSH/GSSG showed about 2-fold decrease relative to the control (Fig. 6). More interestingly, a comparison of Fig. 4A with Fig. 6 clearly indicates that the reactive oxygen species generation and collapse of the redox buffering system mediated by **1a** occur almost simultaneously. The results also indicated that there was a relationship between a burst in reactive oxygen species and collapse of the redox buffering system.

### 3.6. Lipid peroxidation

Plasma membrane plays an important role in the regulation of transmembrane transportation and cellular signaling transduction, as well as the control of cell activation, proliferation and apoptosis (Trouverie et al., 2008). The major components of plasma membrane lipids are the most vulnerable molecules to reactive oxygen species attacking and resulting in lipid peroxidation. Lipid peroxidation was increased as measured the amount of MDA, the biomarker of lipid oxidation. After treatment with **1a** at the

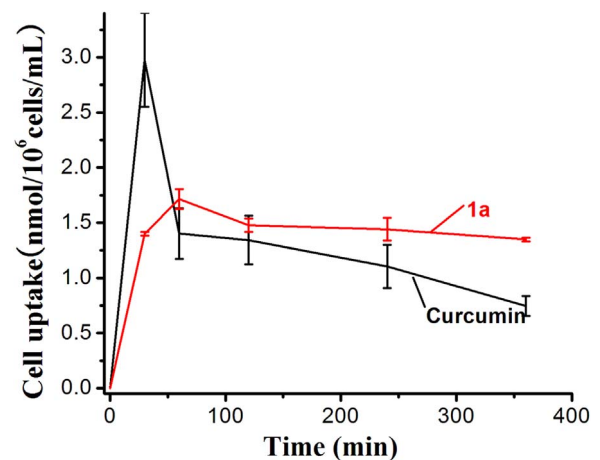


**Fig. 5.** Cellular uptake of curcumin and **1a** (30  $\mu\text{M}$ ) estimated by absorbance measurement of methanol-extracted cell lysates as a function of the incubation period.

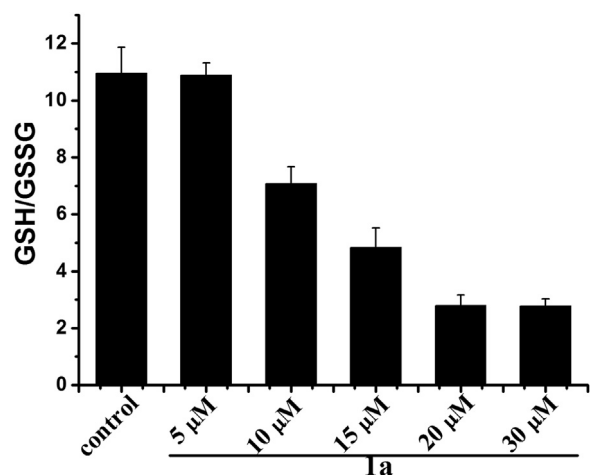


**Fig. 6.** Imbalance of redox homeostasis induced by **1a** in NCI-H460 cells. The GSH/GSSG ratios in cells after treatment with **1a** at the indicated concentrations for 6 h. Each experiment was performed in triplicate.

indicated concentrations, we found that the malondialdehyde levels were sharply increased in a dose-dependent fashion. In particular, after treatment with 30  $\mu\text{M}$  **1a** against NCI-H460 and A549 cells, the amount of MDA with a 3-fold and 2-fold increase

relative to the control, respectively (Fig. 7A and B). These results suggest that cell lipid peroxidation was induced by **1a** may be via the intracellular reactive oxygen species accumulation.

### 3.7. The collapse of mitochondrial membrane potential (MMP)

The loss of mitochondrial membrane potential is a characteristic feature of metazoan apoptosis and has been observed to play a key role in drug-induced death in protozoans such as *Leishmania* (Klaunig and Kamendulis, 2004). In order to determine the apoptosis induced by **1a** involved the mitochondrial, we monitored the changes on mitochondrial membrane potential with Rhodamine 123 by flow cytometry. As shown in Fig. 8A and B, we found that **1a** was more active than the leading curcumin at the indicated concentrations in the collapse of mitochondrial membrane potential. The results indicated that treatment of **1a** against NCI-H460 and A549 cells triggers the reduction of MMP. As expected, pretreatment with GSH or NAC for 1 h, the collapse of mitochondrial membrane potential can be significantly blocked. The results also demonstrate that the collapse of mitochondrial membrane potential was closely related with the reactive oxygen species generation promoted by **1a**.

## 4. Discussions

Curcumin, a nature cancer chemopreventive agent, possesses a surprising array of biological and pharmacological stems from its molecular structure and functionality. It is striking that the curcumin analogs, shortening of the C<sub>7</sub> linker to a C<sub>5</sub> linker results in compounds, not only enhance their bioavailability but also exhibit more active than the leading curcumin (Liang et al., 2009). Our group's work was also exploiting the feasibility in designing curcumin-inspired anticancer agent by a prooxidant strategy, and found that they can target TrxR and convert this antioxidant enzyme into a reactive oxygen species promoter (Dai et al., 2015). Additionally, fluorine is a prominent element in marketed drugs and development candidates. The introduction of fluorine into a molecule can productively influence conformation, pKa, intrinsic potency, membrane permeability, metabolic pathway, and pharmacokinetic properties (Hagmann, 2008). However, the SAR and mechanism of mono-carbonyl curcumin with fluorine substituted groups attaching to 2-, 3- or 4- position has not been clearly defined.

In this study, we synthesized three fluorine-substituted mono-carbonyl curcumin analogs and evaluated their biological activities. The cytotoxicity of all the three curcumin analogs against NCI-H460 cells were stronger than that of curcumin after

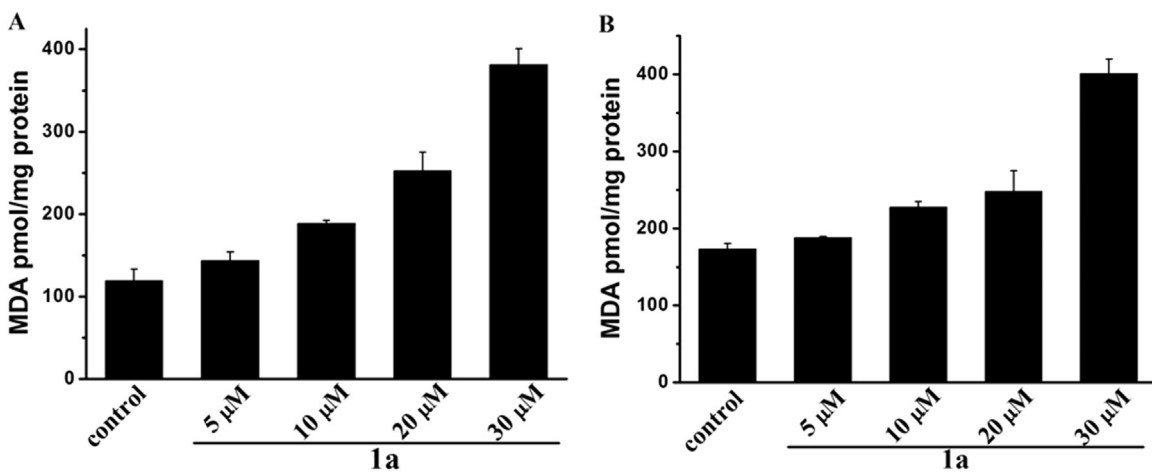


Fig. 7. MDA concentrations of NCI-H460 (A) or A549 (B) cells was determined after exposure to **1a** at the indicated concentrations for 18 h. Values are expressed as MDA equivalents (pmol)/ mg protein. Each experiment was performed in triplicate.

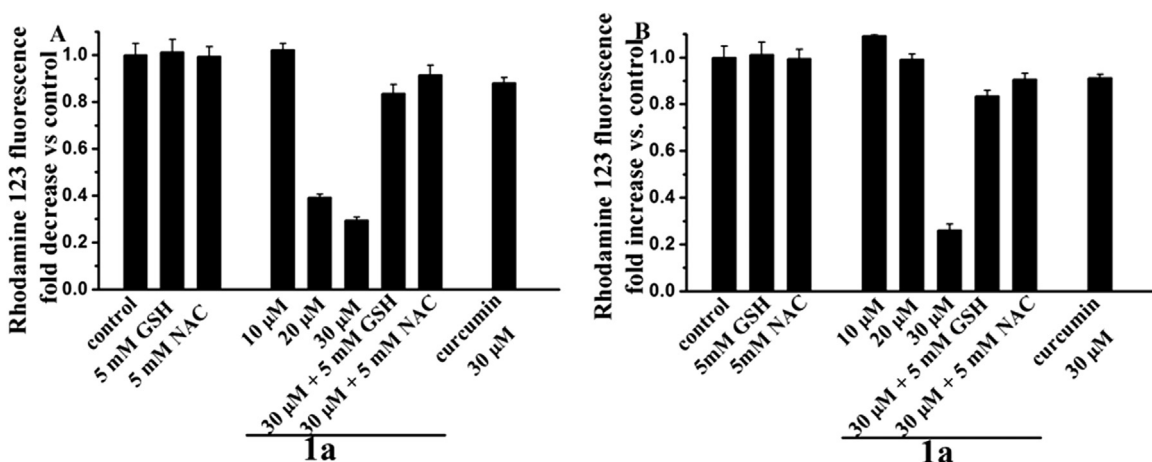
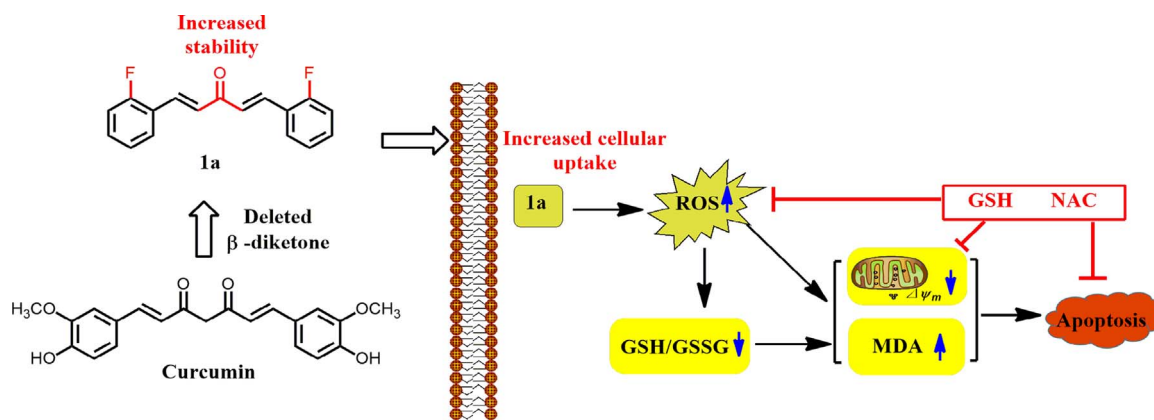


Fig. 8. Effects of GSH (5 mM) and NAC (5 mM) on the collapse of mitochondrial membrane potential induced by **1a** at the indicated concentrations in NCI-H460 (A) or A549 (B) cells for 18 h. Each experiment was performed in triplicate.



**Scheme 1.** 2,2'-Fluorine curcumin causes apoptosis in NCI-H460 cells through reactive oxygen species-Mediated pathway.

treatment for 48 h. Whereas, after treatment for 24 h, curcumin was more activity than all the mono-carbonyl analogs. This paradox phenomenon may be due to the cellular uptake of **1a** and curcumin (Fig. 5). Especially, **1a**, the curcumin analogs with the *ortho*-substituent on the aromatic ring(s), has the best cytotoxicity among all the compounds, this may be due to a so-called *ortho* effect (Dai et al., 2015). However, curcumin and its analogs showed no selectivity against HepG2 and normal Chang's liver cells (Table 1). This may be due to that curcumin and its analogs can suppress multiple signaling pathway and inhibit cell proliferation (Ravindran et al., 2009).

Next, we investigated the mechanism by which **1a** induces cancer cells apoptosis. Many studies have demonstrated that intracellular reactive oxygen species generation is intimately associated with apoptotic cell death (Pelicano et al., 2004; Dai et al., 2015; Ravindran et al., 2009). **1a** can cause a substantial increase in the reactive oxygen species levels in a dose-dependent fashion. More importantly, the reactive oxygen species generation, the collapse of the mitochondrial membrane potential and the apoptosis, which induced by 30  $\mu\text{M}$  **1a** in NCI-H460 and A549 cells, can be almost completely reduced by pretreatment with GSH and NAC. This may indicate that the cytotoxicity and apoptosis-inducing activity of **1a** was closely related to the reactive oxygen species-generating ability. Additionally, we also found that **1a** can disrupt the intracellular redox balance (Dai et al., 2015), induce lipid peroxidation. Interestingly, **1a** was more stable in (RPMI)-1640 medium and more massive uptake than curcumin, this was consistent to their cytotoxicity, apoptotic activity and reactive oxygen species generation. This result also hinted that the more cytotoxicity, apoptotic activity and reactive oxygen species generation of **1a** may be due to its more stable and massive uptake than curcumin.

In conclusion, we synthesized three fluorine-substituted mono-carbonyl curcumin analogs and evaluated their cytotoxicity against normal Chang's liver cells and several cancer cells. The results exhibited that **1a**, the curcumin analogs with the *ortho*-substituent on the aromatic ring(s) significantly increase the cytotoxicity. Mechanistic investigation reveals that the compound could effectively promote the reactive oxygen species generation. The reactive oxygen species generation is associated with falling apart in the redox buffering system, and subsequently induces lipid peroxidation, collapse of the mitochondrial membrane potential, ultimately lead to apoptosis (Scheme 1). The stronger activities of **1a** may be origin from its more stable in (RPMI)-1640 medium and more massive uptake in NCI-H460 cells than curcumin. The results not only suggest that **1a** may cause cancer cells apoptosis through reactive oxygen species-Mediated pathway, but also offer an important information for designing mono-carbonyl curcumin analog with *ortho* effect.

## Acknowledgments

This work was supported by the Doctoral Fund of LiaoCheng University (Grant no. 318051521).

## Appendix A. Supplementary material

Supplementary data associated with this article can be found in the online version at <http://dx.doi.org/10.1016/j.ejphar.2016.06.009>.

## References

- Adams, B.K., Ferstl, E.M., Davis, M.C., Herold, M., Kurtkaya, S., Camalier, R.F., Hollingshead, M.G., Kaur, G., Sausville, E.A., Rickles, F.R., Snyder, J.P., Liotta, D.C., Shoji, M., 2004. Synthesis and biological evaluation of novel curcumin analogs as anti-cancer and anti-angiogenesis agents. *Bioorg. Med. Chem.* 12, 3871–3883.
- Adams, B.K., Cai, J., Armstrong, J., Herold, M., Lu, Y.J., Sun, A., Snyder, J.P., Liotta, D.C., Jones, D.P., Shoji, M., 2005. EF24, a novel synthetic curcumin analog, induces apoptosis in cancer cells via a redox-dependent mechanism. *Anti-Cancer Drugs* 16, 263–275.
- Agrawal, D.K., Mishra, P.K., 2010. Curcumin and its analogues: potential anticancer agents. *Med. Res. Rev.* 30, 818–860.
- Amolins, M.W., Peterson, L.B., Blagg, B.S.J., 2009. Synthesis and evaluation of electron-rich curcumin analogues. *Bioorg. Med. Chem.* 17, 360–367.
- Anand, P., Thomas, S.G., Kunnumakkara, A.B., Sundaram, C., Harikumar, K.B., Sung, B., Tharakan, S.T., Misra, K., Priyadarsini, I.K., Rajasekharan, K.N., Aggarwal, B.B., 2008. Biological activities of curcumin and its analogues (Congeners) made by man and Mother Nature. *Biochem. Pharmacol.* 76, 1590–1611.
- Anand, P., Kunnumakkara, A.B., Newman, R.A., Aggarwal, B.B., 2007. Bioavailability of curcumin: problems and promises. *Mol. Pharm.* 4, 807–818.
- Baldwin, P.R., Reeves, A.Z., Powell, K.R., Napier, R.J., Swimm, A.I., Giesler, K., Bommaris, B., Shinnick, T.M., Snyder, J.P., Liotta, D.C., Kalman, D., 2015. Mono-carbonyl analogs of curcumin inhibit growth of antibiotic sensitive and resistant strains of *Mycobacterium tuberculosis*. *Eur. J. Med. Chem.* 92, 693–699.
- Červinková, Z., Křiváková, P., Lábajová, A., Roušar, T., Lotková, H., Kučera, O., Endlicher, R., Červinka, M., Drahotka, Z., 2009. Mechanisms participating in oxidative damage of isolated rat hepatocytes. *Arch. Toxicol.* 83, 363–372.
- Chen, J., He, Z.M., Wang, F.L., Zhang, Z.S., Liu, X.Z., Zhai, D.D., Chen, W.D., 2016. Curcumin and its promise as an anticancer drug: an analysis of its anticancer and antifungal effects in cancer and associated complications from invasive fungal infections. *Eur. J. Pharmacol.* 772, 33–42.
- Cheng, A.L., Hsu, C.H., Lin, J.K., Hsu, M.M., Ho, Y.F., Shen, T.S., Ko, J.Y., Lin, J.T., Lin, B.R., Ming-Shiang, W., Yu, H.S., Jee, S.H., Chen, G.S., Chen, T.M., Chen, C.A., Lai, M.K., Pu, Y.S., Pan, M.H., Wang, Y.J., Tsai, C.C., Hsieh, C.Y., 2001. Phase I clinical trial of curcumin, a chemopreventive agent, in patients with high-risk or pre-malignant lesions. *Anticancer Res.* 21, 2895–2900.
- Chew, E.-H., Nagle, A.A., Zhang, Y., Scarmagnani, S., Palaniappan, P., Bradshaw, T.D., Holmgren, A., Westwell, A.D., 2010. Cinnamaldehydes inhibit thioredoxin reductase and induce Nrf2: potential candidates for cancer therapy and chemoprevention. *Free Radic. Biol. Med.* 48, 98–111.
- Dai, F., Liu, G.Y., Li, Y., Yan, W.J., Wang, Q., Yang, J., Lu, D.L., Lin, D., Zhou, B., 2015. Insights into the importance for designing curcumin-inspired anticancer agents by a prooxidant strategy: the case of diarylpentanoids. *Free Radic. Biol. Med.* 85, 127–137.
- Fu, Y., Zheng, S., Lin, J., Ryerse, J., Chen, A., 2008. Curcumin protects the rat liver

- from CCl<sub>4</sub>-caused injury and fibrogenesis by attenuating oxidative stress and suppressing inflammation. *Mol. Pharmacol.* 73, 399–409.
- Gan, F.-F., Kaminska, K.K., Yang, H., Liew, C.-Y., Leow, P.-C., So, C.-L., Tu, L.N., Roy, A., Yap, C.W., Kang, T.S., Chui, W.K., Chew, E.H., 2013. Identification of Michael acceptor-Centric pharmacophores with substituents that yield strong thiorodoxin reductase inhibitory character correlated to antiproliferative activity. *Antioxid Redox Signal.* 19, 1149–1165.
- Gazal, M., Valente, M.R., Acosta, B.A., Kaufmann, F.N., Braganhol, E., Lencina, C.L., Stefanello, F.M., Ghisleni, G., Kaster, M.P., 2014. Neuroprotective and antioxidant effects of curcumin in a ketamine-induced model of mania in rats. *Eur. J. Pharmacol.* 724, 132–139.
- Hagmann, W.K., 2008. The many roles for fluorine in medicinal chemistry. *J. Med. Chem.* 51, 4359–4369.
- ICH Harmonised Tripartite Guideline, Q1A(R2), 2003. Stability Testing for New Drug Substance and Products.
- Klaunig, J.E., Kamendulis, L.M., 2004. The role of oxidative stress in carcinogenesis. *Annu. Rev. Pharmacol. Toxicol. Annu. Rev. Pharmacol. Toxicol.* 44, 239–267.
- Kunnumakkara, A.B., Anand, P., Aggarwal, B.B., 2008. Curcumin inhibits proliferation, invasion, angiogenesis and metastasis of different cancers through interaction with multiple cell signaling proteins. *Cancer Lett.* 269, 199–225.
- Liang, G., Shao, L., Wang, Y., Zhao, C., Chu, Y., Xiao, J., Zhao, Y., Li, X., Yang, S., 2009. Exploration and synthesis of curcumin analogues with improved structural stability both in vitro and in vivo as cytotoxic agents. *Bioorg. Med. Chem.* 17, 2623–2631.
- López-Lázaro, M., 2008. Anticancer and carcinogenic properties of curcumin: Considerations for its clinical development as a cancer chemopreventive and chemotherapeutic agent. *Mol. Nutr. Food Res.* 52, S103–S127.
- Pelicano, H., Carney, D., Huang, P., 2004. ROS stress in cancer cells and therapeutic implications. *Drug Resist. Updat.* 7, 97–110.
- Ravindran, J., Prasad, S., Aggarwal, B.B., 2009. Curcumin and cancer cells: how many ways can curry kill tumor cells selectively? *AAPS J.* 11, 495–510.
- Reuter, S., Eifes, S., Dicato, M., Aggarwal, B.B., Diederich, M., 2008. Modulation of anti-apoptotic and survival pathways by curcumin as a strategy to induce apoptosis in cancer cells. *Biochem. Pharmacol.* 76, 1340–1351.
- Sharma, R.A., Steward, W.P., Gescher, A.J., 2007. Pharmacokinetics and pharmacodynamics of curcumin. *Mol. Targets Ther. Uses Curcumin Health Dis.*, 453–470.
- Syng-ai, C., Kumari, A.L., Khar, A., 2004. Effect of curcumin on normal and tumor cells: Role of glutathione and bcl-2. *Mol. Cancer Ther.* 3, 1101–1108.
- Trouverie, J., Vidal, G., Zhang, Z., Sirichandra, C., Madiona, K., Amiar, Z., Prioul, J.L., Jeannette, E., Rona, J.P., Brault, M., 2008. Anion channel activation and proton pumping inhibition involved in the plasma membrane depolarization induced by ABA in *Arabidopsis thaliana* suspension cells are both ROS dependent. *Plant Cell Physiol.* 49, 1495–1507.
- Vandeputte, C., Guizon, I., Genestie-Denis, I., Vannier, B., Lorenzon, G., 1994. A microtiter plate assay for total glutathione and glutathione disulfide contents in cultured/isolated cells: performance study of a new miniaturized protocol. *Cell Biol. Toxicol.* 10, 415–421.
- Weber, W.M., Hunsaker, L.A., Abcouwer, S.F., Deck, L.M., Vander Jagt, D.L., 2005. Anti-oxidant activities of curcumin and related enones. *Bioorg. Med. Chem.* 13, 3811–3820.